J Ther Eng, Vol. 9, No. 2, pp. 297–312, March 2023

Journal of Thermal Engineering
Web page info: https://jten.yildiz.edu.tr
DOI: 10.18186/thermal.1283203

Journal of Thermal Engineering

Research Article

Combined effect of upstream ramp and effusion cooling in combustion chamber liners of gas turbine

Yellu KUMAR[1], Adnan QAYOUM[1,*], Shahid SALEEM[1], Fasil QAYOUM MIR[2]

[1]*Mechanical Engineering Department, National Institute of Technology Srinagar, J&K, 190006, India*
[2]*Chemical Engineering Department, National Institute of Technology Srinagar, J&K, 190006, India*

ARTICLE INFO

Article history
Received: 12 October 2021
Accepted: 10 January 2022

Keywords:
Effusion Cooling; Adiabatic Effectiveness; Blowing Ratio; Upstream Ramp; Combustion Chamber Liners

ABSTRACT

Effusion cooling technique is a highly efficient cooling method used to reduce the thermal stresses of combustion chamber liners in a gas turbine engine. The present study focuses on enhancing the adiabatic effectiveness of effusion cooling. The computational investigations are carried out using COMSOL Multiphysics 5.4 with the standard k- ε turbulence model. Detailed computations for 20 rows of effusion holes on the flat plate are examined for blowing ratios 0.25, 0.5, 1.0, 3.2, and 5.0 for each set of injection angles 30° and 60°. To enhance the effusion cooling performance, an upstream ramp (ramp angles 14°, 24°, and 34°) is introduced before the upstream of effusion holes. The results show that the adiabatic effectiveness increases with an increase of blowing ratio and ramp angles. By placing an upstream ramp, the low blowing ratios can greatly increase the adiabatic effectiveness by 29%, 31%, and 35% for ramp angles of 14°, 24°, and 34°, respectively. For high blowing ratios, an increase in the angles of the ramp shows less impact on adiabatic effectiveness throughout the effusion surface. However, adiabatic effectiveness has increased by 26% compared to the baseline model. It is also observed that injection angle of 30° provides more effectiveness than 60°. This study concludes that placing an upstream ramp increases the effusion cooling performance in the combustion chamber liners of a gas turbine engine.

Cite this article as: Kumar Y, Qayoum A, Saleem S, Qayoum Mir F. Combined effect of upstream ramp and effusion cooling in combustion chamber liners of gas turbine. J Ther Eng 2023;9(2):297–312.

INTRODUCTION

In gas turbine and aero-engines, attempts have been made for many decades to achieve optimum thermal efficiency and power output [1-4]. To enhance the overall efficiency of a gas turbine, extremely high inlet temperatures and pressure ratios are needed, which raises the temperature and pressure in the combustion chambers of gas turbine engines. As a result, a combustion chamber may be subjected to temperature in the range of 1200°C to 1500°C.

***Corresponding author.**
*E-mail address: adnan@nitsri.ac.in

This paper was recommended for publication in revised form by Regional Editor Muslum Arici

Published by Yıldız Technical University Press, İstanbul, Turkey

On account of this high temperature, combustion liners have to act as a protective layer between the hot gases within the combustion chamber and the exterior casing of the combustion chamber. This has led to new research studies in the combustion chamber design for increased performance of the gas turbine system. One such study involves cooling of the combustion chamber liners in order to reduce thermal cracks, structure failures and increasing the reliability of the overall system.

Different cooling strategies are used to reduce the surface temperatures of hot components inside the gas turbine mainly: film cooling, effusion cooling, transpiration, and impingement cooling. Effusion cooling is well suited for combustion chamber liners. A secondary fluid/ cold gas is injected through a large number of small, inclined holes by forming a coolant film on the surface, which protects as a thermal shield between the hot gas flow and wall [1]. The performance of an effective effusion cooling is determined by geometrical parameters like hole diameter (d), hole injection angle (α), spacing of holes in both streamwise (S_x) and spanwise (S_y) directions, length to diameter ratio (L/d), etc., flow parameters like momentum flux (I), blowing ratio (BR), velocity ratio (VR), density ratio (DR), and Reynolds number (Re) etc.., and thermal conductivity of base material [5,6]. Research is being carried out related to effusion cooling performance experimentally and numerically since the last few decades. Because of the high manufacturing costs and technical challenges, the experimental investigations are carried out on flat plates with simple geometry in small-scaled wind tunnels, like real combustion chambers. As it is difficult to conduct experimental investigations on an actual combustion chamber sector, computational simulations, using advanced computational fluid dynamics (CFD) methods, with a combination of heat transfer tools to optimize the overall performance of effusion cooling, is a promising alternative.

Gaustafsson [7] explained the effect of velocity ratio and temperature ratio on effusion cooling performance over a flat plate surface at injection angle of 30° and blowing ratio of 0.89. The author concluded that change in the blowing ratio had little effect on the effusion surface temperature for plates with sparse hole spacing, but a significant effect for dense spacings of holes and the same coolant mass flow rate. Martin and Thorpe [8] conducted studies on an effusion test plate with an inclined holes array with a staggered pattern, adjusting the blowing ratios within the range of 0.3 to 1.5, under conditions of very high freestream turbulence up to 25%. Due to the spanwise lateral spreading of coolant and the turbulent transport of coolant back towards the effusion plate surface, they discovered that increasing freestream turbulence could increase spatially averaged efficacy by as much as 85 % at blowing ratio (BR) of 1.4. Lin *et al.* [9] studied the effusion cooling performance with different cooling patterns. They found that the most important parameters affecting the overall efficiency is hole injection angle and spacing of holes. Also studied the impact of blowing ratio on forward and reverse injection holes. Andreini *et al.* [10] conducted the experimental investigation on seven perforated flat plates with different design aspects such as hole diameter and spacing of holes at different flow parametric conditions, blowing ratio ranging 0.5-5, density ratio 1 and 1.15 and turbulence levels 1.5% and 17%. Baldauf *et al.* [11] measured the local adiabatic effectiveness and heat transfer coefficient on a flat plate by varying geometrical parameters and flow conditions. If large blowing ratios are used, a small pitch between the adjacent holes cannot be attained, steeper blowing angles provide a better heat flux reduction than shallow angle ejection. A high blowing ratio can impart additional heat stresses to the surface. Martiny *et al.* [12] calculated adiabatic effectiveness over the effusion surface with low injection angle of 17° by varying blowing ratios. They have observed different flow patterns at different blowing ratios. Lamyaa and Deborah [13] studied error values by comparing the standard k-ε turbulence model with the Yang-Shih turbulence model using experimental data from a cross-flow with varying angled impact jet holes. Silieti *et al* [14] used five turbulence models to explore film cooling over a flat surface: the standard k-ε model, the realizable k-ε model, the RNG k-ε model, the standard k-ω model, and the SST k-ω model. In the downstream zone, it was found that the standard k-ε turbulence model predicted close conformance to experimental results for the center line adiabatic effectiveness.

The present study involves enhancing the adiabatic cooling effectiveness of effusion cooling by varying the geometric and flow parameters, based on the gaps in the literature. It has been seen from the research that use of cylindrical/ other shaped holes having injection angles in the range of 30°-60° at different flow conditions form a thick film layer protecting the surface. A proper thermal shield protection is possible only when the coolant remains close to the surface without penetrating the mainstream flow. Such ideal situation/condition never occurs even in the most efficient cooling system on account of the vortices (usually the shape of a kidney) generated when coolant is injected through the holes into the mainstream. To circumvent such issues, research on changing geometrical parameters or involving reduction in the kidney-shaped vortex or combination of both, is being pursued. Gritsch *et al.* [15] reported that the improvement of adiabatic effectiveness and increase of lateral spread of coolant flow over the surface can be obtained by providing an expanded exit at the hole. Zaman and Foss [16] placed a tab near the hole's exit to weaken the kidney vortices by reducing the penetration of coolant jet into the mainstream flow and increasing the lateral spread of coolant over the surface. Qayoum et al [17-19] carried out experimental investigation of synthetic jet in cross flow interaction with laminar/turbulent boundary layer. A maximum enhancement of 44%, of heat transfer coefficient, was achieved on account of the ring vortex content in the jet

being deflected towards the wall while merging with the main flow. Na and Shih [20] investigated numerically the effect of placing an upstream ramp in front of the cooling holes to study the boundary layer and coolant flow interactions. The investigation was carried out by varying the ramp angles, blowing ratios and the distance between the backward face of ramp and cooling hole. Nisar *et al.* [21] showed that placing tabs on the coolant hole's upstream and downstream edge increases the adiabatic effectiveness. This reduces the jet lift-off and increases the lateral spreading of jet. Haven and Kurosaka [22] introduced a pair of vanes into the coolant jet hole, rather than the hole's exit, to weaken the kidney vortices by forming cancelling vortices such that the coolant jet attaches to the surface. Barogozzi *et al.* [23] investigated the effect of placing an upstream ramp in front of cylindrical and fan-shaped holes. In case of cylindrical holes for low blowing ratio, the upstream ramp increases thermal protection by nearly 40%. Still, there is a decrease of adiabatic effectiveness for all blowing ratios for the fan-shaped holes. Chen *et al.* [24] studied the effect of an upstream ramp by placing the ramp in front of coolant holes by varying blowing ratios. They reported that the film cooling effectiveness in the downstream region of cooling holes is sensitive to the blowing ratio and height of the backstep of the ramp.

Literature shows that exhaustive research has been carried out for enhancement of cooling performance by modifying geometrical and flow parameters through effusion cooling involving interaction of jet with the main flow. However efficient configuration for improvements of the adiabatic effectiveness in the front rows of the holes for effusion cooling is still lacking. This can be circumvented by placing a ramp on the upstream of the effusion holes. The objective of the present study involves the investigation of the combined effect of the upstream ramp and blowing ratio on the effusion cooling of the combustion liners.

MATERIAL AND METHOD

Governing Equations

The numerical analysis is carried out using Reynolds averaged Navier-Stoke (RANS) equation involving standard k-ε turbulence model for 3-dimensional, steady, incompressible and turbulent flow. The equations involved are:

Continuity Equation:

$$\rho\nabla.(u) = 0 \tag{1}$$

Momentum Equation:

$$\rho(u.\nabla)u = \nabla.[-\mathrm{pI}] + (\mu + \mu_t)\nabla u + (\nabla u)^t - \frac{2}{3}\rho kI + F] \tag{2}$$

where $\mu_t = \rho C_\mu \frac{k^2}{\varepsilon}$

Energy Equation:

$$\rho C_p\, u.\nabla T = -\nabla.(\mathrm{k}\nabla T) + Q \tag{3}$$

where μ is dynamic viscosity, μ_t is turbulent viscosity due to velocity fluctuations, ρ□ is the fluid density, **u** is the velocity component in the computational domain, **p** is fluid pressure field and **F** is volume force field.

To define the physical interface the standard *k*-ε turbulence model involves the following dependent variables i.e. turbulent kinetic energy (*k*) and turbulent dissipation rate (ε).,

Turbulent kinetic energy equation (k):

$$\rho(u\cdot\nabla)k = \nabla\cdot\left[\left(\mu + \frac{\mu_t}{\sigma_k}\right)\nabla k\right] + P_k - \rho\varepsilon \tag{4}$$

Dissipation equation (ε):

$$\rho(u\cdot\nabla)\varepsilon = \nabla\cdot\left[\left(\mu + \frac{\mu_t}{\sigma_\varepsilon}\right)\nabla\varepsilon\right] + Ce_1\frac{\varepsilon}{k}P_k - Ce_2\rho\frac{\varepsilon^2}{k} \tag{5}$$

where,

$$P_k = \mu_t[\nabla u : (\mu + \nabla\mu_t)] + \frac{2}{3}\rho k\nabla\cdot u$$

$$C_\mu = 0.09 \quad \sigma_k = 1 \quad \sigma_\varepsilon = 1.3 \quad Ce_1 = 1.44 \quad Ce_2 = 1.92$$

where C_μ, σ_k, σ_ε, Ce_1 and Ce_2 are some adjustable *k*-ε model constants.

Computational Details and Model

The computational investigation is carried out using Commercial CFD software, COMSOL Multiphysics 5.5 to solve 3-dimensional, steady, compressible, and turbulent flow. The standard k-ε turbulence model is used to simulate the flow field. Literature shows that the standard k-ε turbulence model can accurately predict the surface temperature distribution over the flat surface [3,4]. A typical k-ε turbulence model has been reported to effectively estimate the centerline adiabatic effectiveness of film cooling [13,14]. The standard wall function is applied in the near wall region. The viscous clustering value y+ is maintained at 7 near the solid walls. The symmetrical boundary conditions are applied in the normal direction (Z) to reduce the numerical efforts and computation time. The schematic of computational model is shown in Figure 1.

The Figure 1 consists of mainstream flow, coolant flow and effusion plate with 20 rows of inclined holes in streamwise direction. The circular holes are arranged in a staggered pattern. The hole diameter (d) is 5.7 mm, and the coolant is injected into the mainstream flow at injection angles α= 30° and 60°. The thickness of effusion plate is 3mm. The streamwise and spanwise spacing between two adjacent holes is

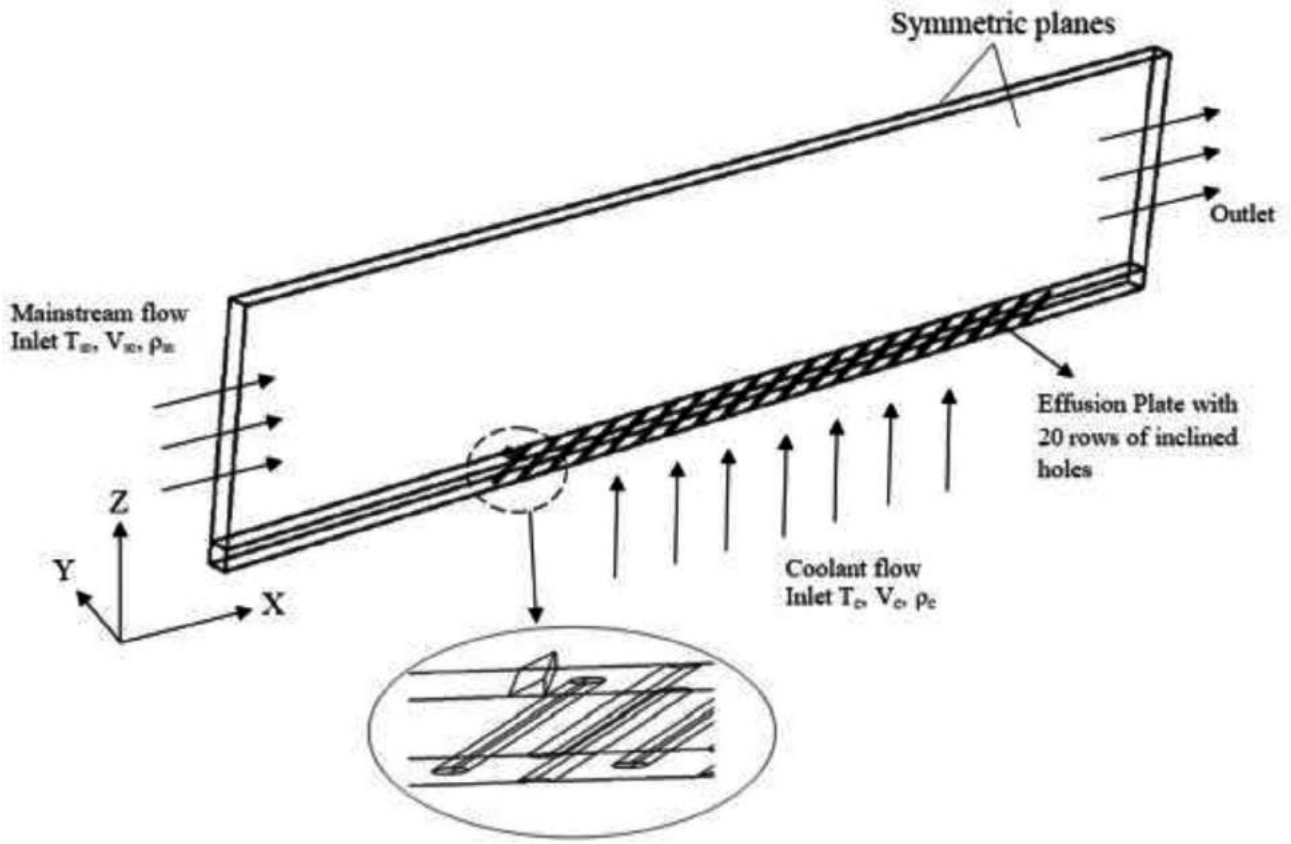

Figure 1. Schematic of computational model.

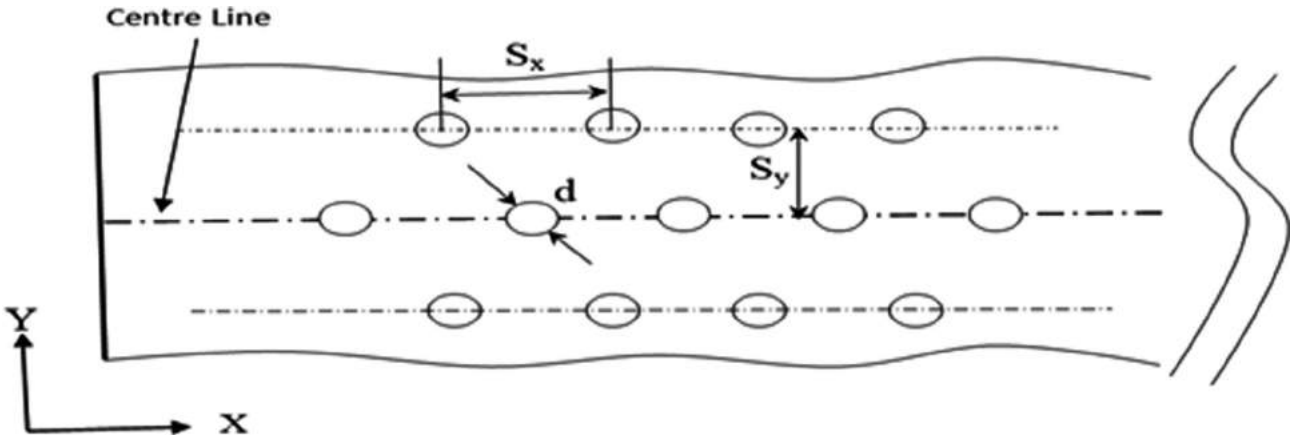

Figure 2. Arrangement of effusion holes in staggered pattern in XY plane (upstream ramp not included).

$S_x/d = S_y/d = 4.9$. The height of the mainstream flow domain in Z-direction is 50d, and the width in Y-direction is 20d. The complete details of the effusion plate are shown in Figure 2. To identify the effect of the upstream ramp on effusion cooling scheme, investigations are carried out on a flat plate with and without the upstream ramp at five different blowing ratios BR= 0.25, 0.5 1, 3.2, and 5.0. The upstream ramp is located at a distance of d from the first row of cooling holes, with a length of 2d. Three ramp angles $\alpha_1 = 14^o$, 24^o, and 34^o are used for an upstream ramp. The schematic

Table.1 List of all possible combinations performed in the present study

S. No / Parameters	Injection angle (α)	Upstream models with ramp angles (α_1)	Blowing ratios (BR)
1	30°	Baseline case (without upstream ramp)	0.25
		Upstream ramp with 14°	0.5
		Upstream ramp with 24°	1.0
		Upstream ramp with 34°	3.2
			5.0
2	60°	Baseline model (without upstream ramp)	0.25
		Upstream ramp with 14°	0.5
		Upstream ramp with 24°	1.0
		Upstream ramp with 34°	3.2
			5.0

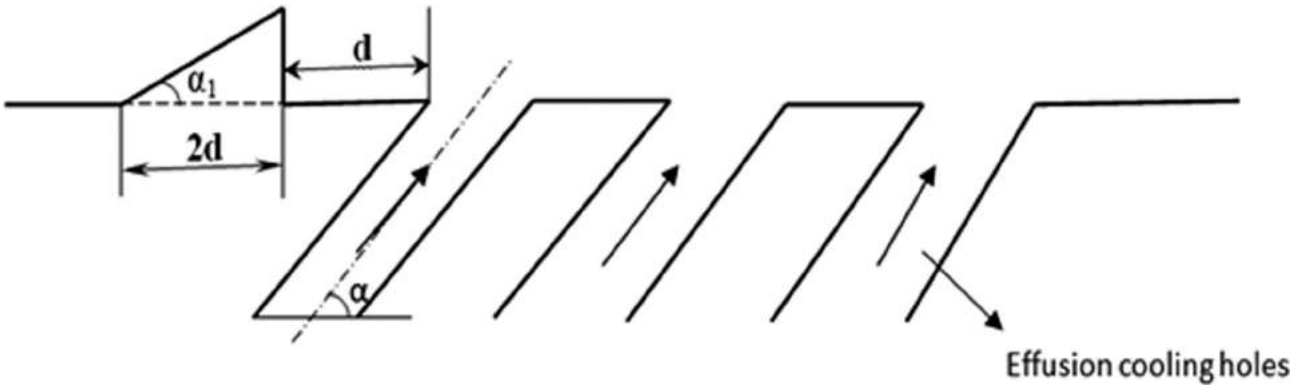

Figure 3. Schematic diagram of an upstream ramp.

of the upstream ramp is shown in Figure 3. A complete list of all the combination of the various parameters used in the investigation are tabulated in Table 1.

Boundary Conditions

The mainstream and coolant flow inlets are specified as velocity inlets, and the outlet is set as a pressure outlet. The inlet velocity of mainstream flow is fixed at V_∞=50 m/s and the coolant flow inlet velocity V_c is calculated according to blowing ratios (BR). The bottom of the effusion plate is treated as a velocity inlet, and the coolant fluid is injected through the effusion holes directly into the mainstream duct. For all the cases, the inlet temperatures of mainstream flow and coolant flow are T_∞= 350K and T_c= 300K resulting in the unit density ratio (DR). The thermal conductivity (k) of the effusion plate is set as 0.027 W/mK so that conduction and internal cooling contributions in effusion holes can be negligible and, hence justifying adiabatic conditions. The turbulence intensity at both inlets is specified as 5%. All the domain walls are subjected to no-slip condition except the interface between effusion plate and mainstream flow. Because of the symmetry of the effusion hole structure on the plate surface, only a small symmetric segment between the two lines of rows (twice of spanwise distance S_y) is selected for computation purposes, as shown in Figure 3. The symmetry planes are applied in the normal direction (Z) for the whole computation domain. The properties of air such as dynamic viscosity, ratio of specific heats and heat capacity at constant pressure are dependent on temperature. A complete list of the geometrical and flow parameters used in the study is tabulated in Table 2.

The effusion cooling performance is measured by term adiabatic effectiveness (η) and this non-dimensionless temperature is defined as [5,6]

$$\eta = \frac{T_\infty - T_{wt}}{T_\infty - T_C} \tag{6}$$

Table 2. Geometrical and flow parameters used in the study.

Geometrical Parameters	Flow parameters
d = 5.7 mm	T_∞ = 350K
t = 3 mm	T_c = 300K
S_x/d = 4.9	V_∞ = 50 m/s
S_y/d = 4.9	V_c = Varied according to the blowing ratios
α = 30° and 60°	
α_1 = 14°, 24° and 34°	Thermal conductivity (k) of the plate = 0.027 W/m.K

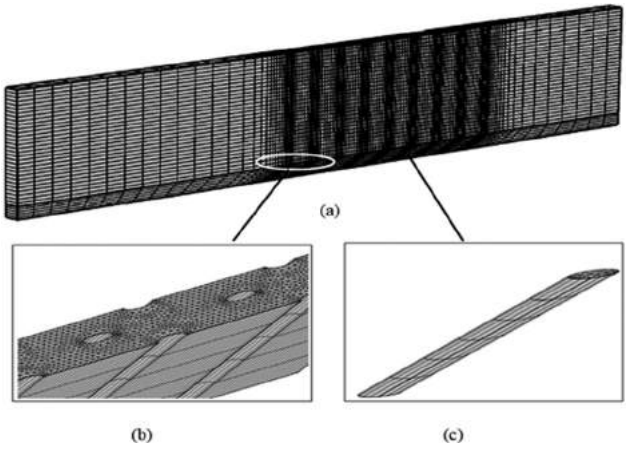

Figure 4. Computational Mesh (a) Entire geometry, (b) Effusion plate surface, and (c) Effusion hole.

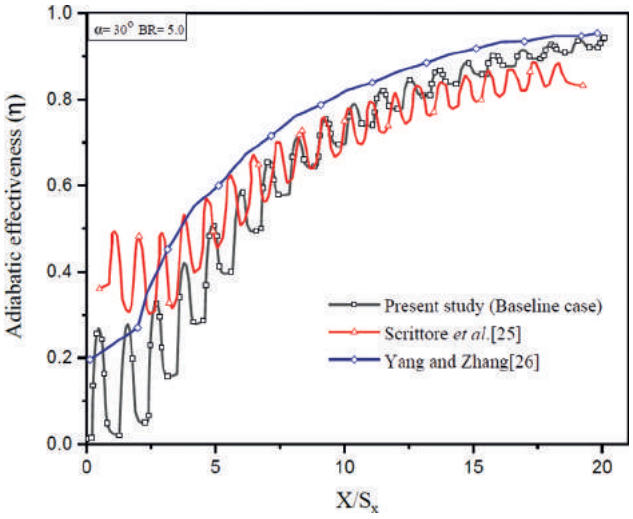

Figure 5. Comparison of centerline adiabatic effectiveness of Computational results with experimental results [25][26] for BR = 5.0 and α = 30°.

where T_∞, T_c and T_{wt} represent the mainstream flow temperatures, the coolant flow and wall temperature on the effusion plate, respectively. The higher value of η indicates that wall temperature on effusion plate surface is low and reduced to a desirable objective. The low value of η indicates improper cooling. The adiabatic effectiveness is measured along the centerline as shown in Figure 2. The parameters that influence the value of η includes blowing ratio (BR) and density ratio (DR) as well as geometrical parameters d, α, S_x and S_y.

The blowing ratio is the ratio of coolant mass flow rate to mainstream flow rate [5].

$$BR = \frac{\rho_C V_C}{\rho_\infty V_\infty} \tag{7}$$

The blowing ratios used in the present study are 0.25, 0.5, 1, 3.2 and 5.0. The values of 0.25, 0.5 are considered low BR, value 1.0 as intermediate BR, and the values 3.2 and 5.0 are high BR.

Density ratio is the ratio between coolant flow density to mainstream flow density.

$$DR = \frac{\rho_C}{\rho_\infty} \tag{8}$$

Grid Distribution and Validation

In this section, a study of grid sensitivity is carried out on a computational model to ensure that the results obtained are independent of the mesh size. The accuracy of the results depends upon grid size. User-controlled mesh sequence is chosen in this study. The effusion plate surface is modelled with free tetrahedral mesh, with fine grid size, to get the high resolutions of the flow parameters variations. The remaining geometry swept mesh, with a fixed number of elements, is distributed on the domains as shown in Figure 4. Grid independence has been investigated for three different grid sizes with 2.2 million (coarse mesh), 2.8 million (fine mesh), and 3.0 million (extremely fine mesh) elements. It was observed that the variation in centerline adiabatic effectiveness over the surface between fine mesh and extremely fine is 7.2%. The present simulation was run on a 2.8 million (fine mesh) to maintain symmetry between computing time economy and efficiency. The number of grid cells varies according to the computational models (varies with ramp angles (α_1) and injection angles (α)). The convergence criteria for residual monitors have been set at 10^{-5}.

To validate the present simulation results, a few validation tests are carried out to measure the centreline adiabatic effectiveness (η) for the effusion cooling scheme. The present computational results are compared with experimental

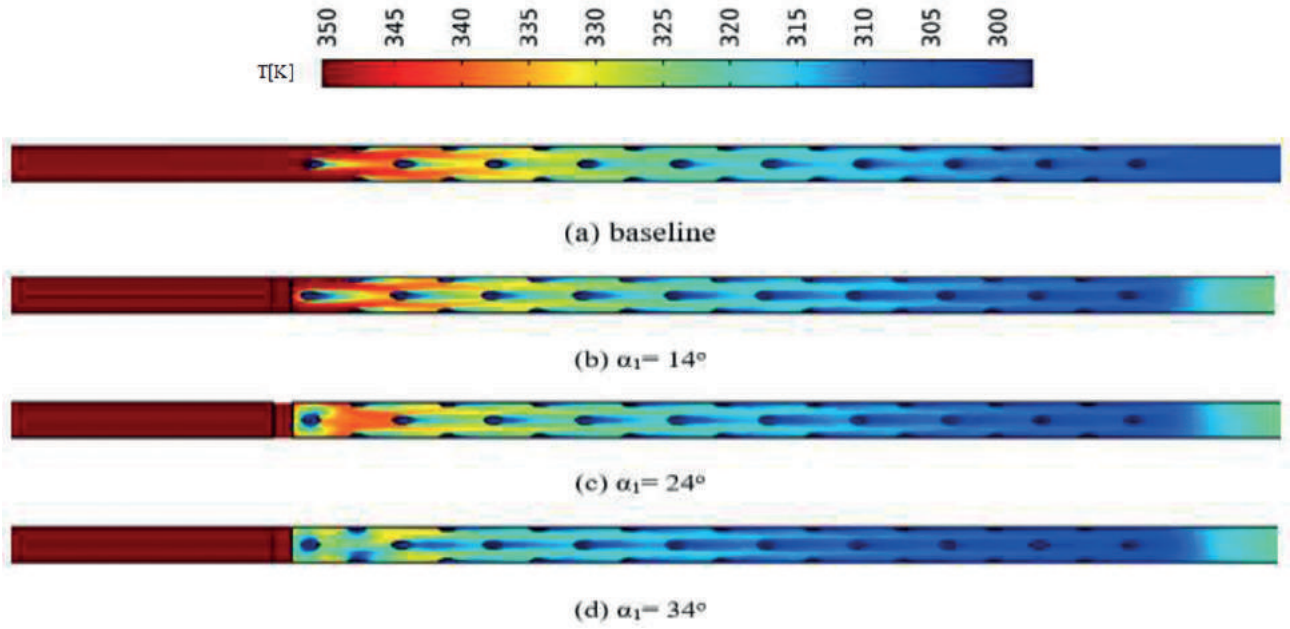

Figure 6. Effusion surface temperature contours in XY plane for injection angle α= 30°, BR= 0.25 at (a) baseline model (b) 14° (c) 24° (d) 34°.

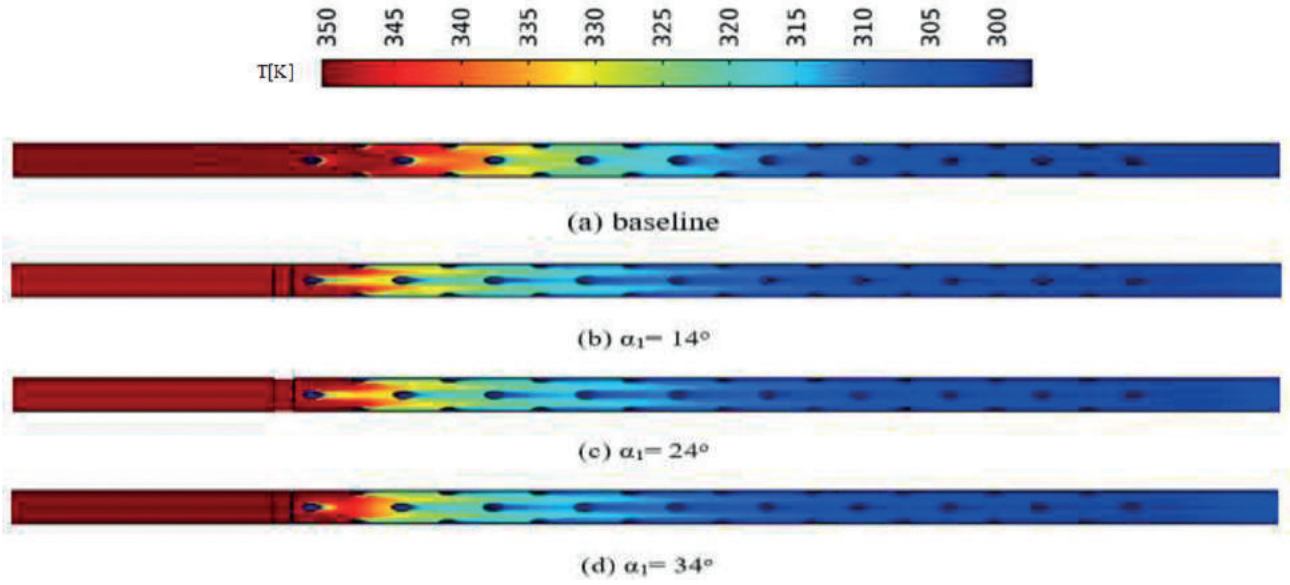

Figure 7. Effusion surface temperature contours in XY plane for injection angle α = 30°, BR = 1.0 at (a) baseline model, (b) 14°, (c) 24°, (d) 34°.

results of Scrittore *et al.* [25] and Yang and Zang [26]. In the study, the flow and geometrical parameters are strictly followed [25]. The Figure 5 shows the comparison of centreline adiabatic effectiveness with experimental results [25][26] for BR= 5.0 and α= 30°. The results show good agreement, except for the first few rows of holes (X/S_x > 3) which may be due to error assuming on the adiabatic approximation on the effusion flat plate. The slight variations between the experimental and computational results arise on account of the fact that during experimentation, perfectly adiabatic conditions are impossible to achieve. The percent error between the experimental results [25] and present computational results, is 5.3%, which is within permissible limit.

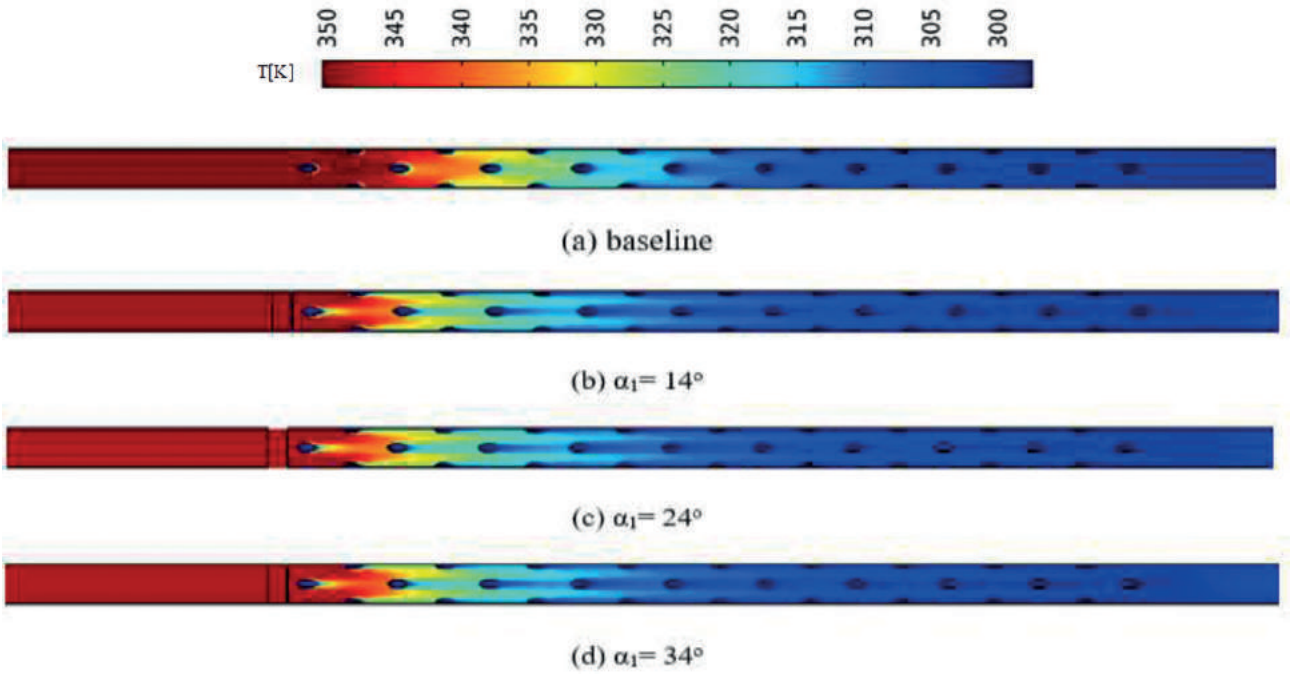

Figure 8. Effusion surface temperature contours in XY plane for injection angle α= 30°, BR = 5.0 at (a) baseline model (b) 14°, (c) 24°, (d) 34°.

RESULTS AND DISCUSSIONS

This section discusses effect of different blowing ratios, geometrical parameters, ramp angles in terms of temperature profiles and adiabatic effectiveness for the liners of the combustion chamber. Adiabatic effectiveness is an important parameter for the performance evaluation of the cooling system. Figure 6, Figure 7, and Figure 8 show the temperature contours T on the effusion plate on the hot-side wall for blowing ratios 0.25, 1.0 and 5.0 for all different ramp angle models. The temperature contours in the three figures corresponds to low blowing ratio (BR = 0.25, intermediate blowing ratio (BR= 1.0 and high blowing ratio (BR= 5.0) at low injection angle (α) = 30°.

The plots of temperature contours show significant variations for all the blowing ratios. As the coolant velocity is low at low blowing ratios (BR= 0.25) the coolant jet remains close to the wall surface without interfering with the mainstream. This is exhibited by the presence of low temperature contours in the initial region (first rows) of the effusion holes (see in Figure 6). With increase in the blowing ratios, the coolant starts penetration into the mainstream. This causes hot gases to reach the surface and is indicated by the high temperature contours being visible in the initial regions (see Figure 7 and Figure 8 corresponding to intermediate and high blowing ratios). The downstream adiabatic effectiveness increases due to accumulation of coolant mass flow rate. Different ramp angles (α_1) of 14°, 24° and 34° are investigated. The effect of ramp is appreciable as is seen by comparison with the baseline case (corresponding to a case without ramp).

Mechanism for Effusion Cooling Improvement by An Upstream Ramp

The flow behind a backward-facing step of the ramp has been extensively studied with promising results in majority of the circumstances in the heat transfer and fluid dynamics involving combustion studies. Figure 9 shows the schematic of the flow pattern behind the upstream ramp. The fluid flow is clearly seen impacted by a high turbulent shear layer separated from the ramp tip with a recirculating zone formed as shown in Figure 9. As separated shear layer increases in the streamwise direction and attaches to the surface, the recirculating region area behind the ramp decreases. Under fully turbulent flow conditions, the reattachment distance is 5-7 times the height of the backward-facing step of the ramp. In the present geometry, the first row of effusion holes is placed at a distance of 1d from the ramp which makes the separated flow field to vary due to ramp height and injection of coolant flow, particularly in the recirculating region. With injection of coolant, the flow in the region will no longer be two-dimensional because the interaction between the coolant flow injection and recirculating region flow generates additional shear layers with a high level of turbulence. Under such conditions, the fluid flow is expected to have more lateral spread over the surface.

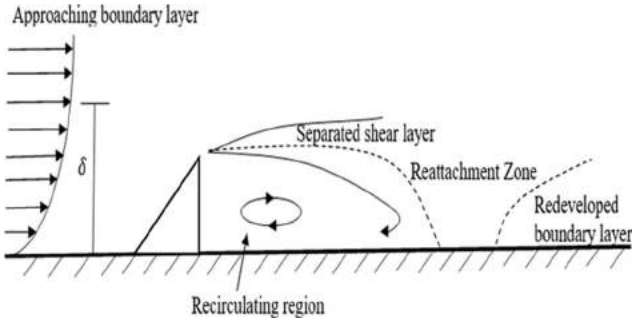

Figure 9. Schematic of flow pattern over an upstream ramp.

Effect of Upstream Ramp on Centerline Adiabatic Effectiveness (η)

Figure10 and Figure 11 show the adiabatic effectiveness distribution on the centerline of the effusion plate for various ramp angles (α_1) at various blowing ratios. As the coolant jet is injected over the surface and interacts with the mainstream flow, the local oscillating peaks occur in each curve. From Figure 10 (a) and 11 (a) for the baseline case, the adiabatic effectiveness is high for the initial (first few rows of holes) for low BR and then decreases in the downward streamwise direction. Unlike these, low values of adiabatic effectiveness are seen at high

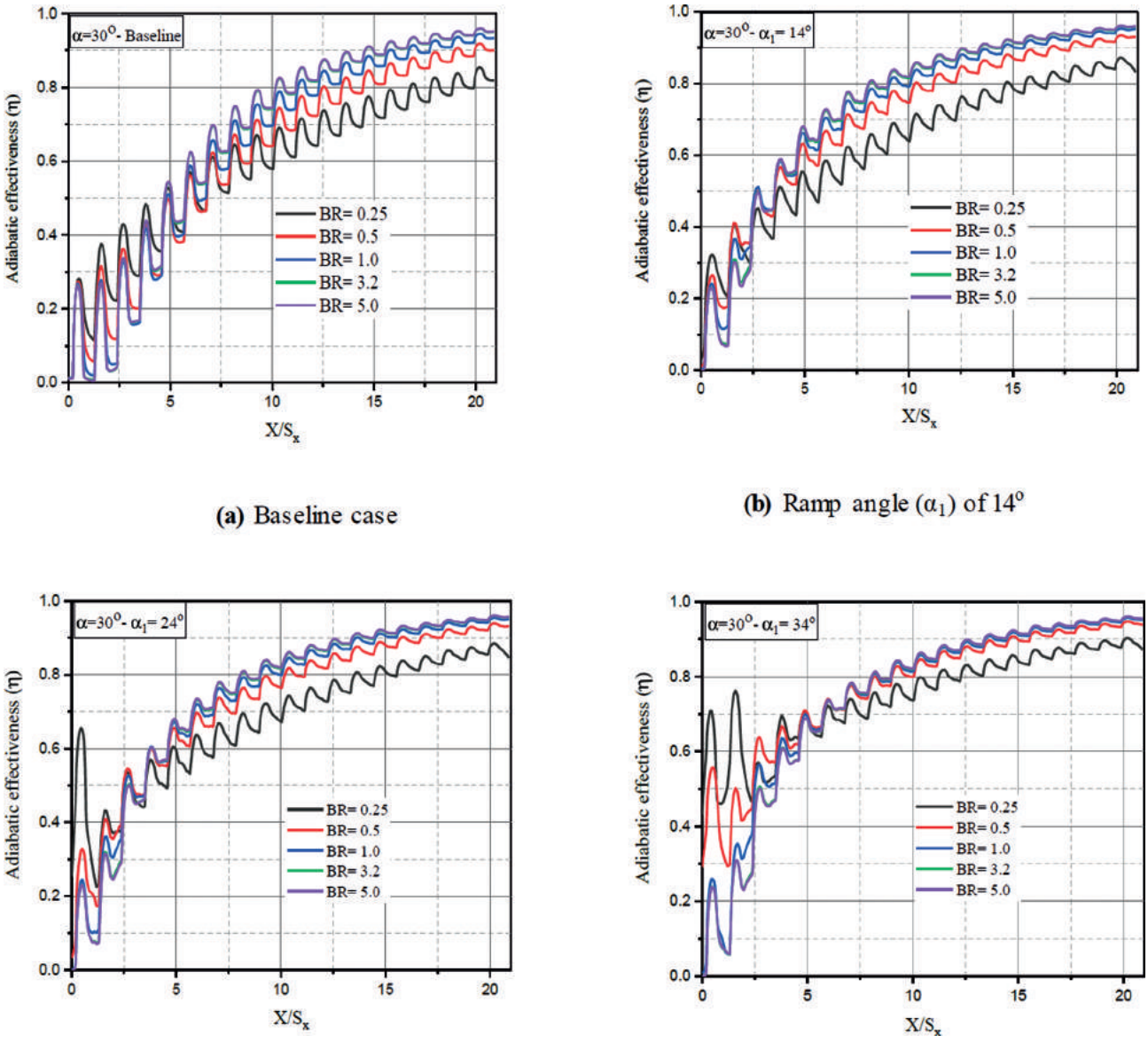

(a) Baseline case

(b) Ramp angle (α_1) of 14°

Figure 10. Comparison of Centerline adiabatic effectiveness for different ramp angles (α_1) at injection angle of 30°.

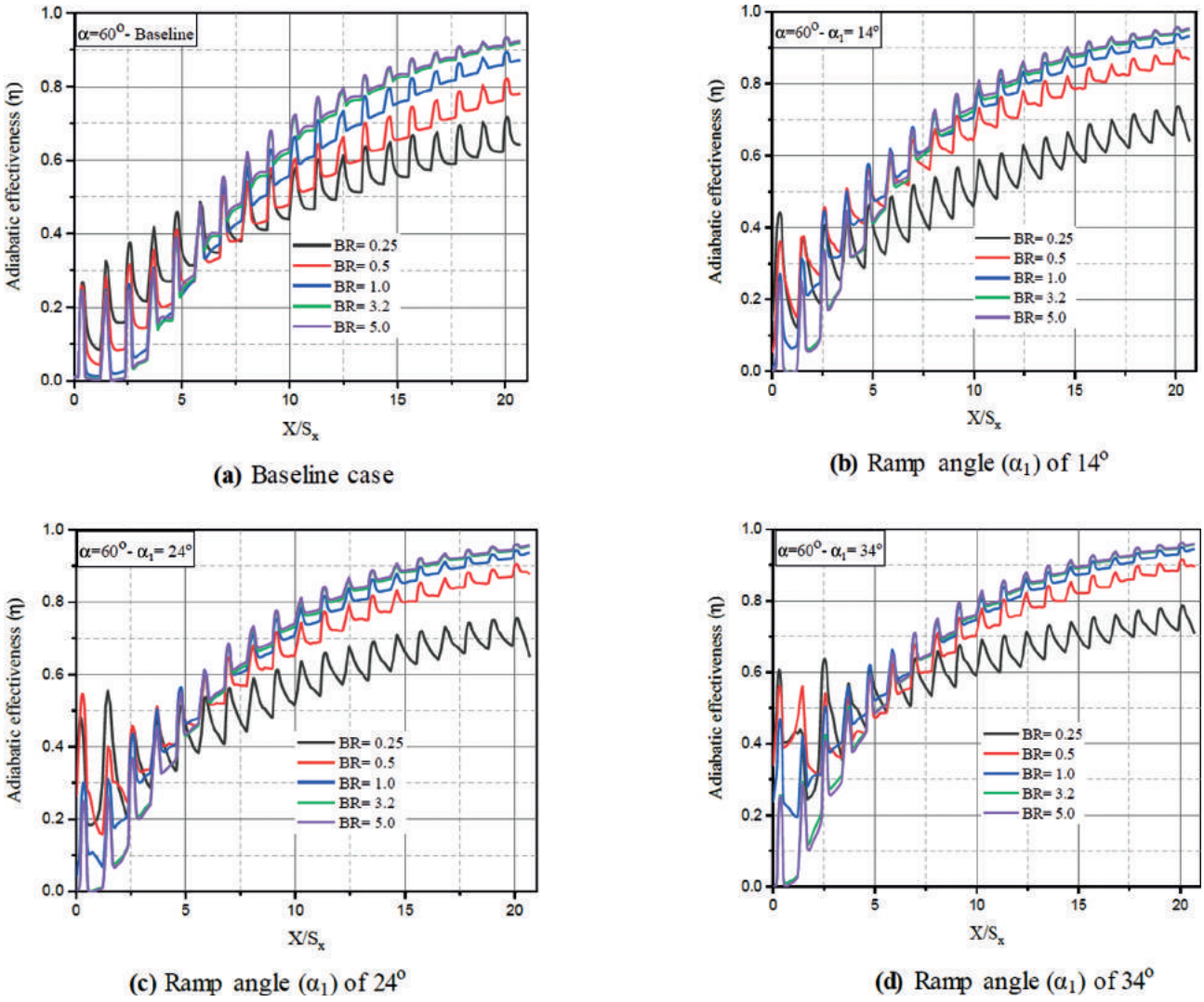

Figure 11. Comparison of Centerline adiabatic effectiveness for different ramp angles (α_1) at injection angle of 60°.

BR = 5.0 for both the baseline cases. This is because for low BR, the coolant jet velocity is very low compared to the mainstream flow velocity which causes the pressure force of approaching boundary layer of mainstream flow to bend the coolant jet towards the effusion surface. As a result, the coolant attaches to the surface in the initial region (first few holes) and thereby causing an increase in adiabatic effectiveness. On the downstream region a thin film of coolant is formed at low BR allowing hot gases to come in contact with the surface and thereby decreasing adiabatic effectiveness by low coolant flow injection (see in Figure 12 (b)). Similar trends are observed by placing an upstream ramp. The adiabatic effectiveness increases as the ramp angle (ramp height) increase and as seen in high effectiveness in the first few rows of holes for every ramp angle. The adiabatic efficiency in the streamwise direction has improved for all blowing ratios due to the placing an upstream ramp.

Figure 10 (b) and 11 (b) shows the comparison of adiabatic effectiveness at ramp angles (α_1) of 14° for two different injection angles (α) of 30° and 60° respectively. The figures show a rapid increase in adiabatic effectiveness in the region X/S_x=0 to X/S_x=5 relative to the baseline case (of Figure 10(a) and Figure 11(a)). This may be due to the entrainment of coolant jet downstream of ramp backward-facing step by the recirculated flow in the separated shear zone. For low BR the lateral spread of the coolant jet increases in this region as the coolant jet does not have enough momentum to penetrate and interact with the mainstream flow. Due to high coolant velocity at high BR, the jet penetrates in the mainstream flow allowing the hot gases to reach the surface and results in decrease in effectiveness. But after the region

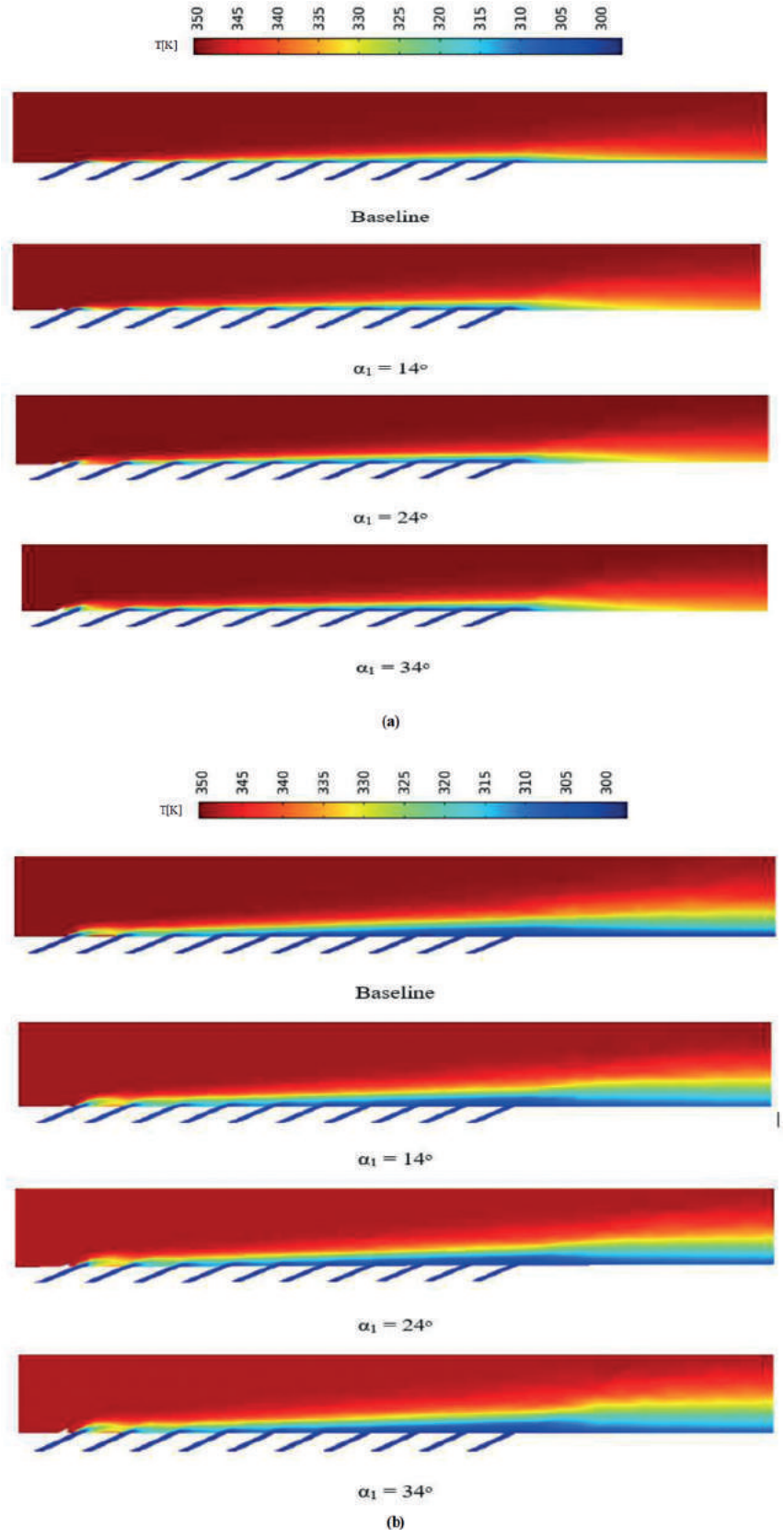

Figure 12. Effusion surface temperature contours in XZ plane for injection angle α= 30° at ramp angles (α_1) of 14°, 24° and 34° for (a) BR=0.25 (b) = 5.0.

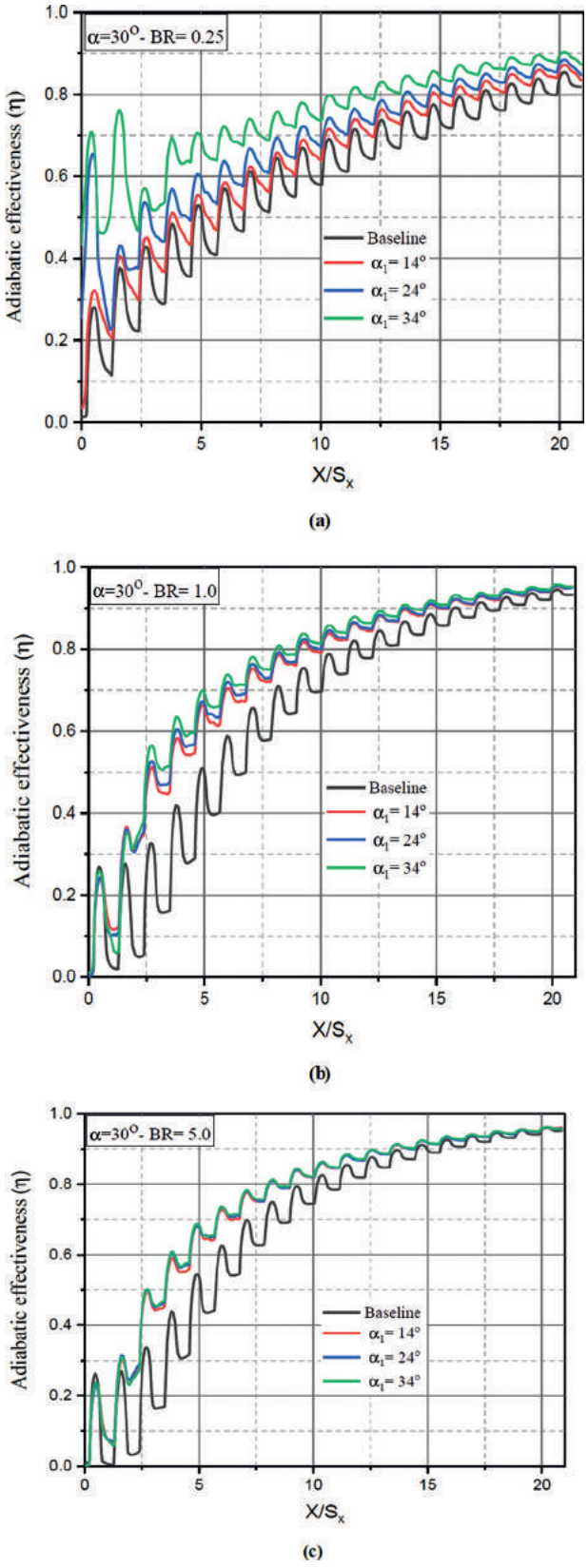

Figure 13. Comparison of Centerline adiabatic effectiveness for different ramp angles at injection angle (α) = 30° (a) BR = 0.25, (b) BR= 1.0 and (c) BR= 5.0.

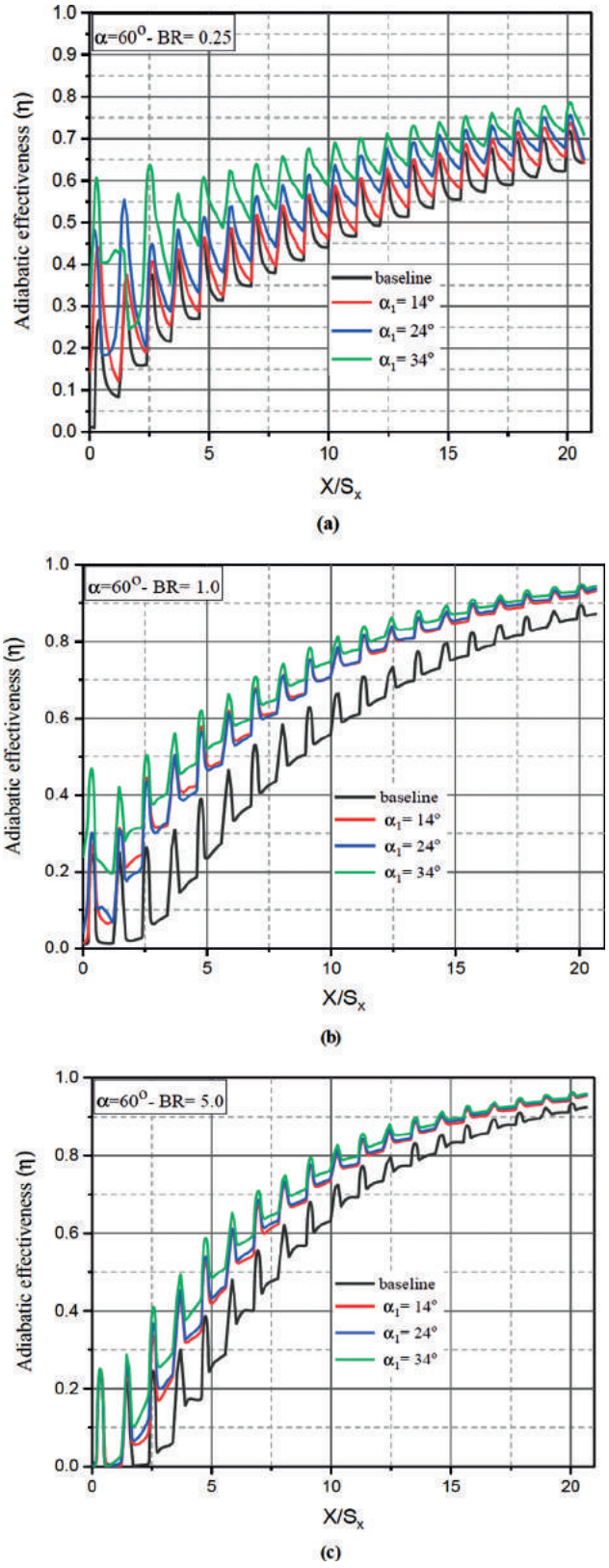

Figure 14. Comparison of Centerline adiabatic effectiveness for different ramp angles at injection angle (α) = 60°, (a) BR = 0.25, (b) BR = 1.0 and (c) BR = 5.0.

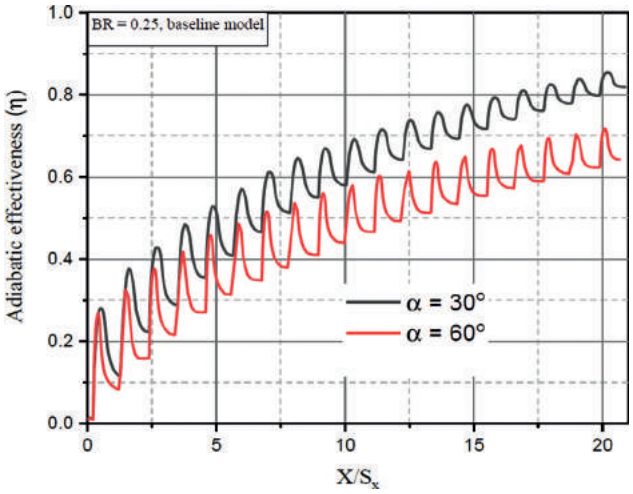

Figure 15. Comparison of Centerline adiabatic effectiveness for different injection angles at BR = 0.25.

X/S_x=5 the adiabatic effectiveness increases for high BR, as discussed earlier. An exponential rise in adiabatic efficiency is observed from Figure 10 (c) (d) for ramp angles 24° and 34°. The reattachment zone increases as the ramp angles (ramp height) expands as the separated shear layer expands. The coolant's lateral spreading is high for low BR in the recirculating area and slightly reduces at high BR. Figure 12 shows surface temperature contours in the XZ-plane for injection angle (α) = 30° at ramp angles (α_1) of 14°, 24° and 34° for different BR of 0.25 and 5.0. With increase in BR, the coolant jet lift-off increases, leading to a decrease in the initial region (first few holes). In the downstream region, due to the high coolant mass flow rate, a thick coolant layer is formed, providing better thermal protection in this zone.

The variations in centerline adiabatic effectiveness for blowing ratios of 0.25, 1 and 5.0 with upstream ramps and baseline for injection angle (α)=30° are shown in Figure 13. Figure 13(a) show large variations in effectiveness between the baseline and upstream ramp cases at low BR. As the ramp angle increases, the adiabatic effectiveness increases throughout the effusion surface, and large variation in adiabatic effectiveness with baseline is observed in the first few rows of holes for BR 0.25 compared to small a variation for the intermediate BR 1.0. However, minor variations are seen due to the ramps and increase in ramp heights. The adiabatic effectiveness in the front row holes is reduced compared to low BR. For high BR 5.0, overall adiabatic effectiveness increases in the downward direction for all the ramp angles and exponential rise in adiabatic effectiveness in the front holes vanishes due to interaction of mainstream flow and coolant jets. The variance in adiabatic effectiveness due to ramps is almost the same. The same behavior is observed for injection angles (α) = 60° (see in Figure 14). It is observed from the Figure 13 (a) for BR= 0.25 at injection angle (α) = 30° in the region X/S_x=0 to X/S_x=5 the adiabatic effectiveness shows an increase of 20%, 55% and 83% for the ramp angles 14°, 24° and 34° respectively compared to baseline model. For the downstream region for X/S_x =5 to X/S_x =20 the effectiveness increases by 6%,10% and 15% respectively for all ramp angles. This is a clear indication that placement of ramp upstream increases the effectiveness in the initial region. The corresponding increases in the adiabatic effectiveness at high BR are 34%, 42% and 46% in the region X/S_x=0 to X/S_x=5 and 4%, 6% and 6% in the region between X/S_x =5 to X/S_x =20. The increase in the effectiveness is relative to the baseline cases. Likewise, Figure 14 shows comparison of centerline adiabatic effectiveness for different ramp angles at injection angle (α) of 60°.

Effect of Injection Angle on Adiabatic Effectiveness

Figure 15 shows comparison of centerline adiabatic effectiveness for different injection angle (α) of 30° and 60° for BR= 0.25. The figure shows that injection angle of 30° provides 19% more effectiveness than angle 60°. This is because the shallower angles allow the coolant flow to stay closer to the surface for more time. The hot gases do not reach the surface as the coolant covers the surface. For higher values of injection angle, the coolant jet penetrates into mainstream flow by increasing the cross mixing of coolant flow and mainstream flow. Hot gases reach the surface for high injection angle thereby decreasing the effectiveness.

Area-Averaged Adiabatic Effectiveness ($\bar{\eta}$)

The Figure16 shows the relation between the blowing ratios and area-averaged adiabatic effectiveness ($\bar{\eta}$) measured on the centerline of the effusion plate for both injection angles of (α) of 30° and 60°. Figure 16 (a) shows that for the baseline case, the area-averaged adiabatic effectiveness (ή) eventually increases for all BRs, and the same behavior is observed for an upstream ramp of (α_1) = 14°. Further increasing the ramp angle (ramp height) i.e., for 24° and 34°, the values of area-averaged adiabatic effectiveness increase as the BR increases from 0.25 to 0.5. Area-averaged effectiveness slightly decreases or is nearly constant with increase in the BR from 0.25 to 0.5. At low BR = 0.25, the area-averaged adiabatic effectiveness ($\bar{\eta}$) is increased to 29%, 31%, and 35% by the upstream ramps at (α_1) of 14°, 24° and 34° respectively as compared with baseline model for injection angles 30°. For blowing ratio 1.0, the area-averaged adiabatic effectiveness has increased by 26%, 27%, and 29% respectively for specified ramp angles and for high BR 5.0, the percentage of increase is 26% for all ramp angles. However, it was observed that the maximum area-averaged effectiveness obtained is 0.747 for BR=1.0, and ramp angle is 34° at injection angle 30°. At a high blowing ratio 5.0 the placement of the upstream ramp has little impact on

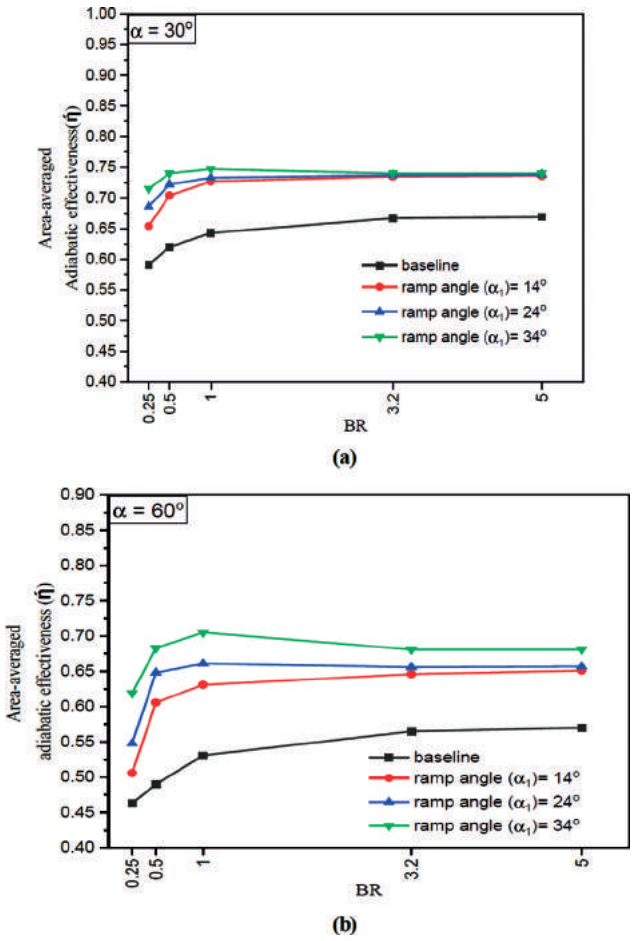

Figure 16. Comparison of area-averaged adiabatic effectiveness vs BR (a) α = 30° (b) = 60°.

the area-averaged effectiveness of effusion cooling performance. This is due to the fact that the coolant velocity at high blowing ratios is substantially higher than the mainstream velocity. The coolant jet penetrates into mainstream flow, allowing hot gases to reach the surface due to rapid interaction of coolant and boundary layer, the low-pressure area generated in the recirculating zone downstream the backward-facing of ramp completely vanishes, lowering the possibility of lateral spreading of the coolant. At the same time a large amount of coolant will be accumulated downstream of the effusion holes, this superposition effect increases the adiabatic effectiveness in the region between X/S_x=5 to X/S_x=20.

Adiabatic effectiveness is influenced by the shape of the holes. In future the effect of various shapes like conical/fan-shaped holes, combined conical-fan-shaped, conical-cylindrical etc. will be investigated. The corresponding effects due to jet issuing for these shapes will be examined in terms of strength of kidney shaped vortices and jet lateral spreads.

CONCLUSIONS

Computational investigations are carried out on the effusion cooling system to enhance the adiabatic effectiveness by placing an upstream ramp in front of the first row of holes. The adiabatic effectiveness is measured and compared with the baseline model for three different ramp angles 14°, 24°, and 34° at various blowing ratios 0.25, 0.5, 1.0, 3.2, and 5.0.

In general, adiabatic effectiveness increases with increase in blowing ratios at all ramp angles. It has been observed that placing an upstream ramp has appreciable impact on the initial region (first few rows of holes, X/Sx <5) compared to the downstream region (X/Sx >5). The values of area-averaged adiabatic effectiveness are low at low blowing ratio of 0.25 which gradually increases up to moderate blowing ratio of 1.0. Increasing blowing ratio beyond this value has insignificant effect on the cooling performance. Ramp angles (ramp height) also influence the adiabatic effectiveness. Low blowing ratios are found to have a strong effect in the initial region (first few holes). The averaged adiabatic effectiveness increases by 29%, 31%, and 35% for low blowing ratio 0.25 and 26% for high blowing ratios 5.0 at different ramp angles of 14°, 24°, and 34°, respectively compared to the baseline model. For high blowing ratios, the change in ramp angles has a minor effect on adiabatic effectiveness. The injection angle (shallower angles) 30° provides better effectiveness than the injection angle (stepper angles) 60°.

NOMENCLATURE

d	[mm]	Diameter of effusion hole
t	[mm]	Thickness of effusion plate
S_x	[mm]	Streamwise distance between hole-to-hole in x-direction
S_y	[mm]	Spanwise distance between hole-to-hole in y-direction
T	[K]	Temperature
V	[m/s]	Flow velocity
X	[mm]	Streamwise coordinate
Y	[mm]	spanwise coordinate
Z	[mm]	Normal coordinate
BR	[-]	Blowing ratio
DR	[-]	Density ratio
VR	[-]	Velocity ratio
I	[-]	Momentum flux ratio
Re	[-]	Reynolds number
K	[W/m.K]	Thermal conductivity
CFD	[-]	Computational Fluid dynamics

Greek letters

α	[°]	Injection angle
α_1	[°]	ramp angle
η	[-]	Adiabatic effectiveness

$\bar{\eta}$	[-]	Area-averaged adiabatic effectiveness
ρ	[kg/m^3]	density

Subscripts

wt	Wall temperature on adiabatic surface of effusion plate
C	Coolant flow
∞	Mainstream flow

AUTHORSHIP CONTRIBUTIONS

Authors equally contributed to this work.

DATA AVAILABILITY STATEMENT

The authors confirm that the data that supports the findings of this study are available within the article. Raw data that support the finding of this study are available from the corresponding author, upon reasonable request.

CONFLICT OF INTEREST

The author declared no potential conflicts of interest with respect to the research, authorship, and/or publication of this article.

ETHICS

There are no ethical issues with the publication of this manuscript.

REFERENCES

[1] Cerri G, Giovannelli A, Battisti L, Fedrizzi R. Advances in effusive cooling techniques of gas turbines. Appl Therm Eng 2007;27:692–698. [CrossRef]

[2] Qayoum A, Panigrahi P. Experimental investigation of heat transfer enhancement in a two-pass square duct by permeable ribs. Heat Transf Eng 2019;40:640–651. [CrossRef]

[3] Rasool A, Qayoum A. Numerical analysis of heat transfer and friction factor in two-pass channels with variable rib shapes. Int J Heat Technol 2018;36:40–48. [CrossRef]

[4] Rasool A, Qayoum A. Numerical investigation of fluid flow and heat transfer in a two-pass channel with perforated ribs. Pertanika J Sci Technol 2018;26:2009–2029.

[5] Kumar KRY, Qayoum A, Saleem S, Qayoum F. Effusion cooling in gas turbine combustion chambers-a comprehensive review. International Symposium on Fusion of Science and Technology; 2020 Jan 6-10; New Delhi, India: IOP Publishing; 2020. Article 012003. [CrossRef]

[6] Krewinkel R. A review of gas turbine effusion cooling studies. Int J Heat Mass Transf 2013;66:706–722. [CrossRef]

[7] Gustafsson KB. Experimental studies of effusion cooling. Gothenburg: Chalmers University of Technology; 2001.

[8] Martin D, Thorpe SJ. Experiments on combustor effusion cooling under conditions of very high free-stream turbulence. Proceedings of ASME Turbo Expo 2012; 2012 Jun 11-15; Copenhagen, Denmark: American Society of Mechanical Engineers; 2012. pp. 1001–1013.

[9] Lin Y, Song B, Li B, Liu G, Wu Z. Investigation of film cooling effectiveness of full-coverage inclined multihole walls with different hole arrangements. Proceedings of ASME Turbo Expo 2003 Power for Land, Sea, and Air; 2003 Jun 16-19; Atlanta, Georgia: American Society of Mechanical Engineers; 2003. pp. 651–660. [CrossRef]

[10] Andreini A, Facchini B, Picchi A, Tarchi L, Turrini F. Experimental and theoretical investigation of thermal effectiveness in multiperforated plates for combustor liner effusion cooling. J Turbomach 2014;136:091003. [CrossRef]

[11] Baldauf S, Scheurlen M, Schulz A, Wittig S. Heat flux reduction from film cooling and correlation of heat transfer coefficients from thermographic measurements at engine like conditions. J Turbomach 2002;36088:163–174. [CrossRef]

[12] Martiny M, Schulz A, Wittig S. Full-coverage film cooling investigations: adiabatic wall temperatures and flow visualization. ASME Paper. Nov 12(95-WA), 1995.

[13] El-Gabry LA, Kaminski DA. Numerical investigation of jet impingement with cross flow—comparison of yang-shih and standard k–ε turbulence models. Numer Heat Transf A Appl 2005;47:441–469. [CrossRef]

[14] Silieti M, Divo E, Kassab AJ. Numerical investigation of adiabatic and conjugate film cooling effectiveness on a single cylindrical film-cooling hole. ASME Int Mech Eng Congress Expo 2004;4711:333–343. [CrossRef]

[15] Gritsch M, Schulz A, Wittig S. Adiabatic wall effectiveness measurements of film-cooling holes with expanded exits. In: The American Society of Mechanical Engineers, editor. Turbo Expo: Power for Land, Sea, and Air. Proceedings Paper. Washington: American Society of Mechanical Engineers.

[16] Zaman KB, Foss JK. The effect of vortex generators on a jet in a cross-flow. Phys Fluids 1997;9:106–114. [CrossRef]

[17] Qayoum A, Gupta V, Panigrahi PK, Muralidhar K. Perturbation of a laminar boundary layer

by a synthetic jet for heat transfer enhancement. Int J Heat Mass Transf 2010;53:5035–5057. [CrossRef]

[18] Qayoum A, Panigrahi PK. Synthetic jet interaction with approaching turbulent boundary layer for heat transfer enhancement. Heat Transf Eng 2015;36:352–367. [CrossRef]

[19] Qayoum A, Gupta V, Panigrahi PK, Muralidhar K. Influence of amplitude and frequency modulation on flow created by a synthetic jet actuator. Sens Actuator A Phys 2010;162:36–50. [CrossRef]

[20] Na S, Shih TP. Increasing adiabatic film-cooling effectiveness by using an upstream ramp. ASME Turbo Expo: Power for Land, Sea, and Air; 2006 May 8-11; American Society of Mechanical Engineers; 2006. pp. 931–938.

[21] Nasir H, Ekkad SV, Acharya S. Flat surface film cooling from cylindrical holes with discrete tabs. J Thermophys Heat Trans 2003;17:304–312. [CrossRef]

[22] Haven BA, Kurosaka M. Improved jet coverage through vortex cancellation. AIAA J 1996;34:2443–2444. [CrossRef]

[23] Barigozzi G, Franchini G, Perdichizzi A. The effect of an upstream ramp on cylindrical and fan-shaped hole film cooling: Part II—Adiabatic effectiveness results. Proceedings of GT2007 ASME Turbo Expo: Power for Land, Sea, and Air; 2007 May 14-17; Montreal, Canada: American Society of Mechanical Engineers; 2007. pp. 115–123. [CrossRef]

[24] Chen SP, Chyu MK, Shih TI. Effects of upstream ramp on the performance of film cooling. Int J Therm Sci 2011;50:1085–1094. [CrossRef]

[25] Scrittore JJ, Thole KA, Burd SW. Investigation of velocity profiles for effusion cooling of a combustor liner. J Turbomach 2007;129:518–526. [CrossRef]

[26] Yang C, Zhang J. Influence of multi-hole arrangement on cooling film development. Chinese J. Aeronaut 2012;25:182–188. [CrossRef]